



HAL
open science

A Constrained Minimal Flavour Violation model facing flavour Physics data

Evan Machefer

► **To cite this version:**

Evan Machefer. A Constrained Minimal Flavour Violation model facing flavour Physics data. Physics [physics]. 2014. dumas-01240491

HAL Id: dumas-01240491

<https://dumas.ccsd.cnrs.fr/dumas-01240491v1>

Submitted on 9 Dec 2015

HAL is a multi-disciplinary open access archive for the deposit and dissemination of scientific research documents, whether they are published or not. The documents may come from teaching and research institutions in France or abroad, or from public or private research centers.

L'archive ouverte pluridisciplinaire **HAL**, est destinée au dépôt et à la diffusion de documents scientifiques de niveau recherche, publiés ou non, émanant des établissements d'enseignement et de recherche français ou étrangers, des laboratoires publics ou privés.



Distributed under a Creative Commons Attribution - NonCommercial - NoDerivatives 4.0 International License



UFR Sciences et Technologies



Laboratoire de Physique Corpusculaire
de Clermont-Ferrand

MASTER SCIENCES DE LA MATIERE DEUXIÈME ANNÉE

SPÉCIALITÉ : Physique des Particules

RAPPORT DE STAGE

A Constrained Minimal Flavour Violation model facing flavour Physics data.

par

Evan MACHEFER

Responsable(s) de stage : **Stéphane MONTEIL**
Jean ORLOFF



Juin 2014

Acknowledgement

I would like to express my gratitude to my supervisors, Stéphane MONTEIL and Jean ORLOFF, for their advices and their remarks that lead me to a better understanding of the subject.

I would like to thank Marouen as well, for sharing his knowledge of subjects unknown to me, that helped me to work in a more efficient way.

Contents

Acknowledgement	iii
Introduction	1
1 CKM matrix and models of Minimal Flavour Violation	3
1.1 CKM matrix and Unitarity Triangles	3
1.1.1 Introduction	3
1.1.2 Number of free parameters	4
1.1.3 Standard parametrisation	5
1.1.4 Wolfenstein parametrisation	5
1.1.5 Unitarity triangles	5
1.2 Minimal Flavour Violation	7
2 Global fits of CKM matrix elements: the LHCb B_s inputs	9
2.1 Preliminary part	9
2.2 Fit for the $(\bar{\rho}_s, \bar{\eta}_s)$ plane	10
3 CMFV in neutral meson mixing	13
3.1 No New Physics at tree-level assumption	13
3.2 Modification of tree-level processes	15
Conclusion	19

Introduction

The Standard Model of particles physics is, so far, the best description there is of the subatomic world, and the recent discovery of a new scalar particle, makes it now complete. It has, for more than sixty years, resisted to all the tests it was submitted to, and one of those tests is the consistency check of the Cabibbo–Kobayashi–Maskawa (CKM) matrix, allowing flavour transitions within weak charged currents. This matrix can be described by four free parameters, that need to be determined by the experiment.

Overconstraining the parameters describing the CKM matrix, one can probe the consistency between the different experiments and the SM expectations. These tests of the CKM matrix are made by two main groups, one is the UTfit collaboration, and the other is the CKMfitter group, whose framework is used hereafter.

CKMfitter is a group of a ten of people gathered to provide worldwide renowned fits, using a minimiser written in fortran, and theories written in the *Mathematica* language.

The first part of this work will focus on the basic knowledge needed to understand what are Constrained Minimal Flavour Violation (CMFV) models, the second part will talk about how new measurements can constrain the CKM matrix elements, and the last part will deal with the CMFV implementation within the CKMfitter package.

Chapter 1

CKM matrix and models of Minimal Flavour Violation

1.1 CKM matrix and Unitarity Triangles

1.1.1 Introduction

The Standard Model (SM) is described by a lagrangian density with a $SU(3)_c \times SU(2)_L \times U(1)_Y$ gauge invariance [1]. In this model, fermions are classified in left-handed doublets and in right-handed chirality singlets.

Gauge invariance forbids mass terms for fermions or gauge bosons. The introduction of a scalar doublet of $SU(2)_L$, denoted ϕ , breaks spontaneously the gauge symmetry when it acquires a vacuum expected value. Conversely, three out of the four scalar fields are absorbed to provide a longitudinal polarisation for the Z and W bosons. At the same time, the ϕ field couples to the quarks by the following most general gauge-invariant and renormalisable Yukawa terms in the lagrangian density:

$$\mathcal{L}_Y = -\lambda_{ij}^d \bar{Q}_{Li}^{I_3} \phi D_{Rj}^{I_3} - \lambda_{ij}^u \bar{Q}_{Li}^{I_3} \epsilon \phi^* U_{Rj}^{I_3} + h.c., \quad (1.1)$$

where $\lambda^{u,d}$ are 3×3 complex mass matrices, ϕ is a scalar $SU(2)$ doublet field, i, j are generation labels, and ϵ is the 2×2 antisymmetric tensor. $Q_L^{I_3}$ are left-handed quark doublets, and U_R, D_R are right-handed singlets in the weak eigenstate basis. When ϕ acquires a vacuum expectation value, $\langle \phi \rangle = (0, v/\sqrt{2})$, mass terms appear

$$-M_{ij}^d \bar{D}_{Li}^{I_3} D_{Rj}^{I_3} - M_{ij}^u \bar{U}_{Li}^{I_3} U_{Rj}^{I_3} + h.c.,$$

with,

$$M^{u(d)} = \frac{\lambda^{u(d)} v}{\sqrt{2}}.$$

The mass matrix can be diagonalised,

$$V_L^{u(d)} M^{u(d)} V_R^{u(d)} = \begin{pmatrix} m_{u(d)} & 0 & 0 \\ 0 & m_{c(s)} & 0 \\ 0 & 0 & m_{t(b)} \end{pmatrix},$$

with $V_L^{u(d)}$ and $V_R^{u(d)}$ unitary matrices. One can then define,

$$Q_{Li}^{I_3} = \begin{pmatrix} U_{Li}^{I_3} \\ D_{Li}^{I_3} \end{pmatrix} = (V_L^{u\dagger})_{ij} \begin{pmatrix} U'_{Lj} \\ (V_L^u V_L^{d\dagger})_{jk} D'_{Lk} \end{pmatrix}.$$

The Cabbibo-Kobayashi-Maskawa (CKM) ([2], [3]) matrix, defined as $V_L^u V_L^{d\dagger}$, is a (3×3) unitary matrix allowing the transition between the flavours of quarks. It relates the weak eigenstates $D^{I_3} = (d, s, b)$ to the mass eigenstates $D' = (d', s', b')$,

$$\begin{pmatrix} d' \\ s' \\ b' \end{pmatrix} = V_L^u V_L^{d\dagger} \begin{pmatrix} d \\ s \\ b \end{pmatrix} = V_{CKM} \begin{pmatrix} d \\ s \\ b \end{pmatrix} = \begin{pmatrix} V_{ud} & V_{us} & V_{ub} \\ V_{cd} & V_{cs} & V_{cb} \\ V_{td} & V_{ts} & V_{tb} \end{pmatrix} \begin{pmatrix} d \\ s \\ b \end{pmatrix}. \quad (1.2)$$

The matrix elements V_{ij} ($i = u, c, t$; $j = d, s, b$) are complex numbers.

1.1.2 Number of free parameters

For an $(n \times n)$ complex matrix, where n describes the number of quark generations, there are $2n^2$ free real parameters, one modulus and one phase for each matrix element. However, for unitary matrices, the relations

$$(VV^\dagger)_{jk} = \sum_i V_{ji} V_{ki}^* = \delta_{jk}, \quad (1.3)$$

where δ_{jk} is the Kronecker delta¹, reduce the number of independent parameters. The compact writing of Eq. (1.3) embodies constraints on real parameters only, such as $|V_{ud}|^2 + |V_{us}|^2 + |V_{ub}|^2 = 1$ ($j = k$), and real and imaginary parts, as in the scalar product between columns $j \neq k$. Eq. (1.3) leads to $n + (n(n-1))/2$ independent constraints on the moduli, and $(n(n-1))/2$ constraints on phases.

Moreover, physics is invariant under

$$V \rightarrow \begin{pmatrix} e^{i\phi_1^U} & & 0 \\ & 0 & \\ 0 & & e^{i\phi_n^U} \end{pmatrix} V \begin{pmatrix} e^{i\phi_1^D} & & 0 \\ & 0 & \\ 0 & & e^{i\phi_n^D} \end{pmatrix},$$

¹ $\delta_{jk} = \begin{cases} 1 & \text{if } i = j \\ 0 & \text{if } i \neq j \end{cases}$

where $\phi_i^{U,D}$ are phases of the up (U) or down (D) mass eigenstate fields.

This rephasing freedom of the $2n$ quark fields can in general be used to fix only $2n - 1$ phases of V , the last rephasing freedom $\phi_i^{U,D} = \phi_{global}$ leaving V unchanged. Thus, the total number of free parameters will be $(n - 1)^2$. The (3×3) CKM matrix depends hence on 4 parameters, one being a phase. The latter implies that CP violation can be accounted for in this framework.

1.1.3 Standard parametrisation

The standard parametrisation [4] for V_{CKM} uses 3 Euler angles (θ_{ij}) and one global phase (δ),

$$V_{CKM} = \begin{pmatrix} c_{12}c_{13} & s_{12}c_{13} & s_{13}e^{-i\delta} \\ -s_{12}c_{23} - c_{12}s_{23}s_{13}e^{i\delta} & c_{12}c_{23} - s_{12}s_{23}s_{13}e^{i\delta} & s_{23}c_{13} \\ s_{12}s_{23} - c_{12}c_{23}s_{13}e^{i\delta} & -s_{23}c_{12} - s_{12}c_{23}s_{13}e^{i\delta} & c_{23}c_{13} \end{pmatrix}, \quad (1.4)$$

where $c_{ij} = \cos(\theta_{ij})$ and $s_{ij} = \sin(\theta_{ij})$.

1.1.4 Wolfenstein parametrisation

In practice, $s_{13} \ll s_{23} \ll s_{12} \ll 1$, and a more convenient way to express V_{CKM} is due to Wolfenstein[5]. The following definitions [6] are adopted:

$$s_{12}^2 = \lambda^2 = \frac{|V_{us}|^2}{|V_{ud}|^2 + |V_{us}|^2}, \quad s_{23}^2 = A^2\lambda^4 = \frac{|V_{cb}|^2}{|V_{ud}|^2 + |V_{us}|^2},$$

$$s_{13}e^{i\delta} = V_{ub}^* = A\lambda^3(\rho + i\eta), \quad \bar{\rho} + i\bar{\eta} = -\frac{V_{ud}V_{ub}^*}{V_{cd}V_{cb}^*},$$

which ensures a parametrisation that is both phase-independent and unitary to all. It can be noted that $\lambda \simeq V_{us}$. For the sake of illustration, Eq. (1.5) shows a truncated expression of V_{CKM} up to $\mathcal{O}(\lambda^4)$,

$$V_{CKM} = \begin{pmatrix} 1 - \lambda^2/2 & \lambda & A\lambda^3(\rho - i\eta) \\ -\lambda & 1 - \lambda^2 & A\lambda^2 \\ A\lambda^3(1 - \rho - i\eta) & -A\lambda^2 & 1 \end{pmatrix} + \mathcal{O}(\lambda^4). \quad (1.5)$$

1.1.5 Unitarity triangles

Two relations coming from Eq. (1.3) will be used in the following,

$$V_{ud}V_{ub}^* + V_{cd}V_{cb}^* + V_{td}V_{tb}^* = 0, \quad (1.6)$$

$$V_{us}V_{ub}^* + V_{cs}V_{cb}^* + V_{ts}V_{tb}^* = 0. \quad (1.7)$$

Notice that the magnitude of each component of Eq. (1.6) is of the same order $\mathcal{O}(\lambda^3)$.

Dividing each term of Eq. (1.6) by $V_{cd}V_{cb}^*$, one obtains,

$$\frac{V_{ud}V_{ub}^*}{V_{cd}V_{cb}^*} + 1 + \frac{V_{td}V_{tb}^*}{V_{cd}V_{cb}^*} = 0. \quad (1.8)$$

Defining then

$$\bar{\rho} + i\bar{\eta} = -\frac{V_{ud}V_{ub}^*}{V_{cd}V_{cb}^*},$$

this sum of three complex numbers can be seen as the closing of an unitary triangle, *i.e.* a triangle with unit basis, in the complex plane $(\bar{\rho}, \bar{\eta})$ as shown in Fig. 1.1. The different parameters displayed are

$$R_u = \left| \frac{V_{ud}V_{ub}^*}{V_{cd}V_{cb}^*} \right|, \quad R_t = \left| \frac{V_{td}V_{tb}^*}{V_{cd}V_{cb}^*} \right|,$$

$$\alpha = \Phi_2 = \arg \left(-\frac{V_{td}V_{tb}^*}{V_{ud}V_{ub}^*} \right), \quad \beta = \Phi_1 = \arg \left(-\frac{V_{cd}V_{cb}^*}{V_{td}V_{tb}^*} \right), \quad \gamma = \Phi_3 = \arg \left(-\frac{V_{ud}V_{ub}^*}{V_{cd}V_{cb}^*} \right).$$

In the following, only the notation (α, β, γ) will be used for the angles.

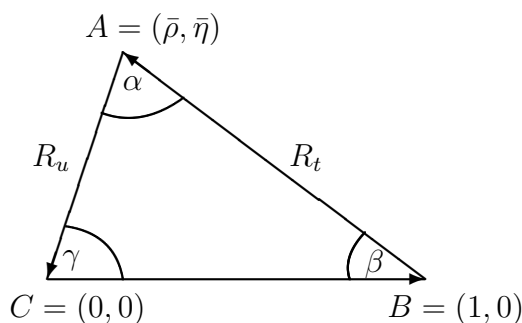


Figure 1.1: Unitary Triangle

We will scrutinise in the section 2.1 the Eq. (1.7) which sides and angles can be obtained from observables related to the B_s meson. With an adequate normalisation, one obtains

$$\frac{V_{us}V_{ub}^*}{V_{cs}V_{cb}^*} + 1 + \frac{V_{ts}V_{tb}^*}{V_{cs}V_{cb}^*} = 0, \quad (1.9)$$

with $\bar{\rho}_s + i\bar{\eta}_s = -\frac{V_{us}V_{ub}^*}{V_{cs}V_{cb}^*}$. Because the terms in this equation have different powers of λ , the corresponding triangle will be squashed, contrarily to the one of Eq. (1.8) related to the B_d meson.

1.2 Minimal Flavour Violation

The Standard Model (SM) describes three out of the four elementary interactions in the framework of gauge theories, and it has not been proven wrong till now. It indeed explains most of the phenomena that have been observed, but it fails at naturally explaining the baryonic asymmetry in the Universe and does not provide a dark matter candidate. The remarkable description of all flavour physics and CP violation observables within the KM framework suggests that any New Physics (NP) model should not bring additional flavour violation beyond that present in the SM. This data-driven assumption defines classes of NP models denoted as Minimal Flavour Violation (MFV).

In MFV models [7], all flavour changing transitions and Charge Parity (CP) violation come from the CKM matrix. The decay amplitudes in MFV models can be written as:

$$A(M \rightarrow F) = P_c(M \rightarrow F) + \sum_r P_r(M \rightarrow F)F_r(v), \quad (1.10)$$

where $F_r(v)$ are real process-independent master functions, that are reduced to the Inami-Lim functions [8] in the SM, and P_c and P_r are process-dependent, but model-independent, coefficients. P_c summarises the light quarks contributions, in particular the charm quark, and P_r in the sum, incorporates the remaining contributions.

The MFV master functions and Inami-Lim functions come from penguin and box diagram computations as the ones shown on Fig. 1.2.

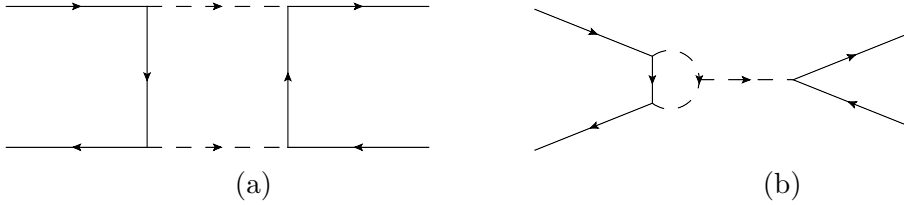


Figure 1.2: Box and penguin diagrams.

Their knowledge is required for the determination of the predictions of the branching fractions. The master functions associated with various processes are given in Table 1.1.

As an example, the branching fraction of $B_s \rightarrow \mu^+ \mu^-$ is given by

$$B(B_s \rightarrow \mu^+ \mu^-) = C |V_{ts} V_{tb}^*|^2 \eta_Y Y(v) \quad (1.11)$$

where η_Y are the QCD corrections, and

$$C = \frac{\tau_{B_s} G_F^2 m_{B_s} m_\mu^2 \alpha_{EM}^2(M_Z)}{16\pi^3 \sin^2 \theta_W \hbar} \sqrt{1 - \frac{4m_\mu^2}{m_{B_s}^2}} f_{B_s}^2. \quad (1.12)$$

$K^0 - \bar{K}^0$ -mixing (ϵ_K)	$S(v)$
$B_{d,s}^0 - \bar{B}_{d,s}^0$ -mixing ($\Delta m_{d,s}$)	$S(v)$
$K \rightarrow \pi \nu \bar{\nu}$, $B \rightarrow X_{d,s} \nu \bar{\nu}$	$X(v)$
$K_L \rightarrow \mu^+ \mu^-$, $B \rightarrow l^+ l^-$	$Y(v)$
$K_L \rightarrow \pi^0 e^+ e^-$	$Y(v), Z(v), E(v)$
ϵ' , Non-leptonic $\Delta B = 1$, $\Delta S = 1$	$X(v), Y(v), Z(v), E(v)$
$B \rightarrow X_S \gamma$	$D'(v), E'(v)$
$B \rightarrow X_S \text{gluon}$	$E'(v)$
$B \rightarrow X_S l^+ l^-$	$Y(v), Z(v), E(v), D'(v), E'(v)$

Table 1.1: The observables related to the master functions.

G_F is the Fermi constant, $\alpha_{EM}(M_Z)$ is the electromagnetic structure constant taken at the mass of the Z boson and f_{B_s} is a form factor, the decay constant, given by lattice QCD computations.

The $Y(v)$ master function absorbs any CMFV constrained NP contributions. Conversely, the v parameter generalises the parameter $x_t = \frac{m_t^2}{M_W^2}$. A specific CMFV model will add up to v the mass dependencies on the hypothetical new particles.

In this paper, the first implementation of CMFV model will focus on the mixing processes, since $S(v)$ is only related to them, as seen on [Table 1.1](#).

Chapter 2

Global fits of CKM matrix elements: the LHCb B_s inputs

2.1 Preliminary part

Before any implementation of CMFV models in the theory packages of CKM-fitter, one should understand how the fit is done. The most simple case, is the fit for the $(\bar{\rho}, \bar{\eta})$ plane using all the standard observables. We have tried to perform a similar fit but using the $(\bar{\rho}_s, \bar{\eta}_s)$ instead.

The result given by CMS and LHCb on the branching ratio of $B_s \rightarrow \mu^+ \mu^-$ [9] gives us information on the $|V_{ts}|$ matrix element. Because it does not give any direct constraint in the $(\bar{\rho}, \bar{\eta})$ plane, it is instructive to implement its effect on a fit in the $(\bar{\rho}_s, \bar{\eta}_s)$ plane instead.

This fit is usually done on $(\bar{\rho}, \bar{\eta})$ plane then transposed to the $(\bar{\rho}_s, \bar{\eta}_s)$ plane, but since $B_s \rightarrow \mu^+ \mu^-$ does not contribute directly in the first, constraint displayed on the latter might suffer from numerical convergency problems. In order to see the constraint of this decay, it is more convenient (but fully equivalent) to re-express all the parameters in terms of $\bar{\rho}_s$ and $\bar{\eta}_s$ instead of $\bar{\rho}$ and $\bar{\eta}$.

From the definition

$$\bar{\rho}_s + i\bar{\eta}_s = -\frac{V_{us}V_{ub}^*}{V_{cs}V_{cb}^*},$$

V_{ub}^* can be extracted in terms of $\bar{\rho}_s$ and $\bar{\eta}_s$:

$$V_{ub}^* = -\frac{A\lambda\sqrt{1-\lambda^2}\sqrt{1-A^2\lambda^4}(\bar{\rho}_s + i\bar{\eta}_s)}{1-A^2\lambda^4(\bar{\rho}_s + i\bar{\eta}_s)}. \quad (2.1)$$

Since $(\bar{\rho} + i\bar{\eta}) = -\frac{V_{ud}V_{ub}^*}{V_{cd}V_{cb}^*}$, $\bar{\rho}$ and $\bar{\eta}$ can in turn be expressed in terms of $\bar{\rho}_s$

and $\bar{\eta}_s$ ¹,

$$\bar{\rho} = \frac{\lambda^2 - 1}{\lambda^2} \frac{\bar{\rho}_s - A^2 \lambda^2 (\bar{\rho}_s^2 + \bar{\eta}_s^2)}{A^4 \lambda^4 \bar{\eta}_s^2 + (1 - A^2 \lambda^2 \bar{\rho}_s)^2}, \quad (2.2)$$

and,

$$\bar{\eta} = \frac{\lambda^2 - 1}{\lambda^2} \frac{\bar{\eta}_s}{A^4 \lambda^4 \bar{\eta}_s^2 + (1 - A^2 \lambda^2 \bar{\rho}_s)^2}. \quad (2.3)$$

Including this change of variables, the fit will be done using $\bar{\rho}_s$ and $\bar{\eta}_s$ instead of $\bar{\rho}$ and $\bar{\eta}$.

2.2 Fit for the $(\bar{\rho}_s, \bar{\eta}_s)$ plane

With the definition given with Eq. (1.9), the $|V_{ts}|$ constraint given by $B(B_s \rightarrow \mu^+ \mu^-) = (2.9 \pm 0.7)10^{-9}$ will lead to a circle centred on $(1, 0)$ as shown on Fig. 2.1.

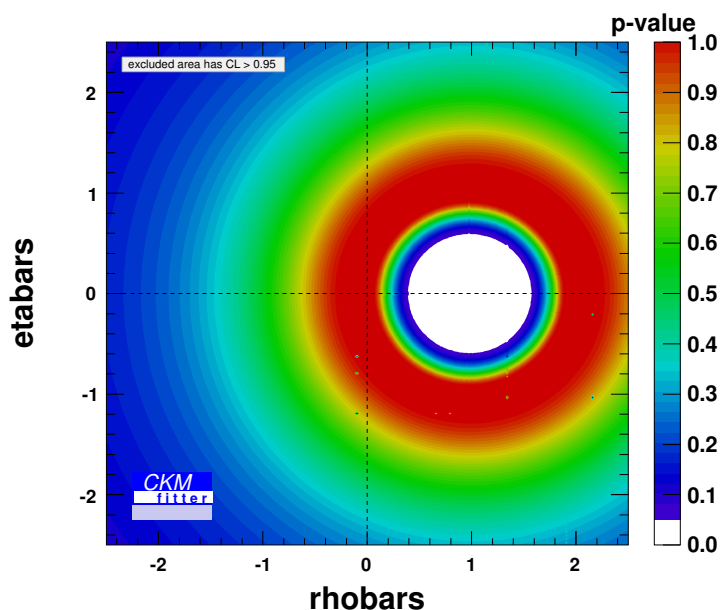


Figure 2.1: Fit of $\bar{\rho}_s, \bar{\eta}_s$ using $|V_{cb}|, |V_{cs}|$ and $B(B_s \rightarrow \mu\mu)$ as inputs.

If $|V_{ud}|$ and $|V_{us}|$ are included as inputs to get a constraint on A and λ , the authorised region will greatly be reduced, only allowing $(\bar{\rho}_s, \bar{\eta}_s)$ to be

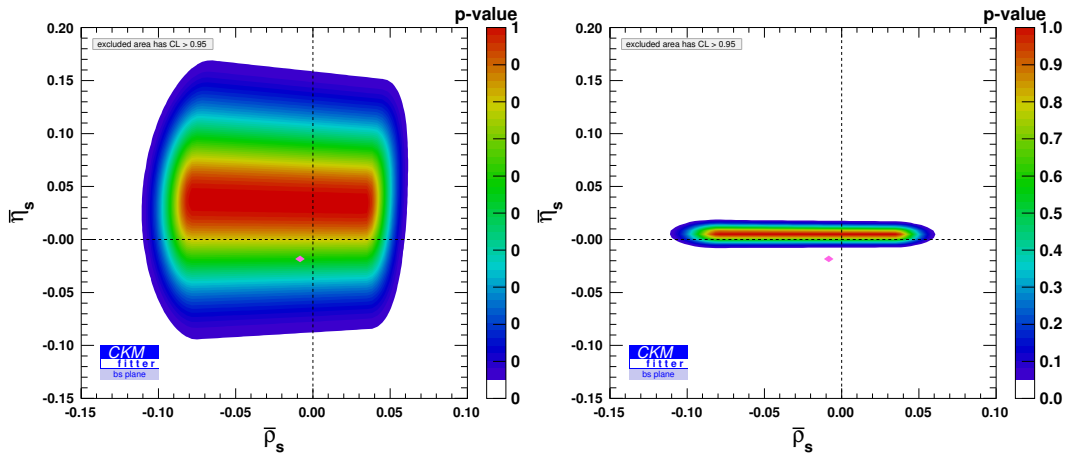
¹This kind of change of variable can also be applied to ρ and η .

2.2. FIT FOR THE $(\bar{\rho}_s, \bar{\eta}_s)$ PLANE

near the origin. The reason is that A and λ greatly constrain $\bar{\rho}_s$ and $\bar{\eta}_s$ due to the relation between $|V_{ts}|$, A and λ :

$$|V_{ts}|^2 = \frac{A\lambda^2}{1 - A^2\lambda^4} [(\bar{\rho}_s - 1)^2 + \bar{\eta}_s^2] |V_{cs}|^2. \quad (2.4)$$

Including also $\Delta m_s = 17.762 \pm 0.023 \text{ ps}^{-1}$, the mass difference in $B_s^0 - \bar{B}_s^0$ mixing, and $\phi_s = 0.01 \pm 0.07 \text{ rad}$, the CP violating phase in B_s^0 decays, in the fit for $(\bar{\rho}_s, \bar{\eta}_s)$ plane, Fig. 2.2a is obtained. With the expected precision



(a) Fit for $\bar{\rho}_s, \bar{\eta}_s$ using ϕ_s , Δm_s and $B(B_s \rightarrow \mu\mu)$ as inputs. The pink dot is the region allowed with the standard fit.

(b) Fit for $\bar{\rho}_s, \bar{\eta}_s$ using the expected precision of ϕ_s , Δm_s and $B(B_s \rightarrow \mu\mu)$ as inputs. The pink dot is the allowed region with the standard fit.

for the LHCb upgrade with the second run of the LHC, $\phi_s = 0.01 \pm 0.01 \text{ rad}$, $\Delta m_s = 17.762 \pm 0.023 \text{ ps}^{-1}$ and $B(B_s \rightarrow \mu^+\mu^-) = (3.0 \pm 0.3)10^{-9}$. A difference between the value of $\bar{\rho}_s$ and $\bar{\eta}_s$ obtained with the usual fit (in pink in Fig. 2.2a and Fig. 2.2b) and the allowed region with ϕ_s , Δm_s and $B(B_s \rightarrow \mu^+\mu^-)$, might occur as shown in Fig. 2.2b. It can be seen that the expected precision of ϕ_s can radically change the allowed region, and that the precision attained with $B(B_s \rightarrow \mu^+\mu^-)$ will not have any effect on the fit.

It is interesting to remark that the precision attained with the fit with B_s^0 systems is not as good as the precision attained with B_d systems related fit.

Chapter 3

CMFV in neutral meson mixing

3.1 No New Physics at tree-level assumption

$B_{d,s}^0 - \bar{B}_{d,s}^0$ oscillations is an effective way to measure the matrix elements $|V_{td}|$ and $|V_{ts}|$ precisely in the framework of the Standard Model. Experimentally, the mass difference between the two states will be measured, Δm_d and Δm_s , for B^0 and B_s^0 respectively, from time-dependent analysis of B oscillations.

In the SM, $\Delta F = 2$ transitions are described by the Inami-Lim function $S_0(x_q)$, with $x_q = m_q^2/M_W^2$. For example, the explicit mathematical expression of a $\Delta S = 2$ transition, as a possible process is shown in Fig. 3.1, is:

$$\text{Box}(\Delta S = 2) = \lambda_i^2 \frac{G_F^2}{16\pi^2} M_W^2 S_0(x_t, x_c) (\bar{s}d)_{V-A} (\bar{s}d)_{V-A}, \quad (3.1)$$

where $\lambda_i = V_{is}^* V_{id}$, ($i = u, c, t$). In fact, that box is linked to the hamiltonian governing the evolution of the $\Delta S = 2$ system.

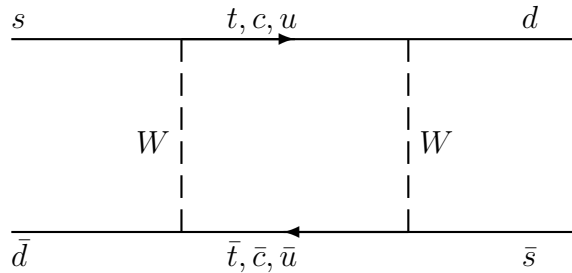
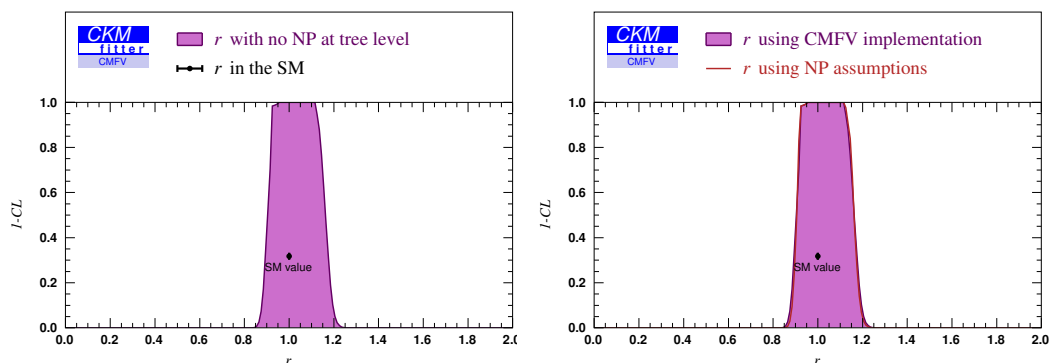


Figure 3.1: Box diagram of a $\Delta F = 2$ transition.

Including CMFV models, one free parameter must be added to describe these mixing. This free parameter is the master function $S(v)$, that will be expressed as $r \times S_0(x_t)$ in the following.

The fit for the r parameter gives us an allowed region for NP that does not exclude the SM, where r is exactly equal to one by definition. The ordinates are the probability value expressed in terms of Confidence Level (CL) of exclusion:

$$\text{p - value} = 1 - \text{CL}$$



(a) Comparison between CMFV implementation in a LO package and the SM point. (b) Comparison between the NP package at NLO and the CMFV implementation at LO.

Figure 3.2: Fit for r using $|V_{ud}|$, $|V_{us}|$, $|V_{ub}|$, $|V_{cb}|$, $\sin 2\beta$, α , γ , Δm_d and Δm_s as inputs.

To test the validity of our implementation, we have compared our results with those of a pre-existing so-called "NP package" [10], where different assumption were made. It must be noticed that, for the sake of the development, the CMFV implementation has been made at Leading Order (LO) (and will be extended to the Next to Leading Order (NLO) at the end of the internship), whereas the "NP package" is at NLO.

In order to be able to compare the two packages, a change of variables must be made for the NP part. The "NP package" is described by six real parameters,

$$\text{Re}(\Delta_d), \text{Re}(\Delta_s), \text{Re}(\Delta_K^{tt}), \text{Im}(\Delta_d), \text{Im}(\Delta_s), \text{Im}(\Delta_K^{tt}),$$

where:

$$\Delta_q = \frac{\langle M_q | H_q^{\text{eff}} | \bar{M}_q \rangle}{\langle M_q | H_q^{\text{SM}} | \bar{M}_q \rangle}, \quad (3.2)$$

with H_q^{eff} the effective hamiltonian of the $M_q - \bar{M}_q$ system ($M_q = B_{d,s}^0, K^0$), and H_q^{SM} the SM hamiltonian. The Δ_q are free parameters added in B^0

mixing, B_s^0 mixing, and K^0 mixing. $B_{d,s}^0$ mixing will be multiplied by $|\Delta_q|$, whereas in ϵ_K , only the top loop will be affected with the term $\mathcal{I}m[(V_{ts}V_{td}^*)^2\Delta_K^{tt}]$. In order to have an equivalent of the r parameter from CMFV, the following assumptions are made:

$$\mathcal{R}e(\Delta_d) = \mathcal{R}e(\Delta_s) = \mathcal{R}e(\Delta_K^{tt}) = r, \quad (3.3)$$

and,

$$\mathcal{I}m(\Delta_d) = \mathcal{I}m(\Delta_s) = \mathcal{I}m(\Delta_K^{tt}) = 0, \quad (3.4)$$

so that no new phase is added, and only one parameter describes NP contributions.

Fig. 3.2b shows that our implementation is compatible with the "NP package", for the same assumptions as in CMFV models.

With the assumption that no NP appears in tree level processes, CMFV deviations of order twenty percent are allowed, as seen in Fig. 3.2a and Fig. 3.2b.

3.2 Modification of tree-level processes

Since there is a tension between inclusive and exclusive determinations of both $|V_{ub}|$ and $|V_{cb}|$, it is worth exploring the possibility that tree level processes are affected by NP as well. Numerically,

$$\begin{aligned} |V_{ub}|_{\text{incl}} &= (4.36 \pm 0.18 \pm 0.44)10^{-3}, & |V_{ub}|_{\text{excl}} &= (3.23 \pm 0.20 \pm 0.26)10^{-3}, \\ |V_{cb}|_{\text{incl}} &= (41.88 \pm 0.44 \pm 0.59)10^{-3}, & |V_{cb}|_{\text{excl}} &= (39.55 \pm 0.51 \pm 1.42)10^{-3}. \end{aligned}$$

These values should then be excluded from the fit in order to see how the allowed region for r is modified with this assumption. Fig. 3.3 shows the effect of relaxing the constraints from $|V_{ub}|$ and $|V_{cb}|$ on the r parameter.

In this fit, the observables $|V_{ud}|$, $|V_{us}|$, the angles α , β , γ , and the meson mixing Δm_d , Δm_s and ϵ_K constrain the free parameters. $|V_{ud}|$ and $|V_{us}|$ are used in $\lambda = \frac{|V_{us}|^2}{|V_{ud}|^2 + |V_{us}|^2}$, hence λ might not be affected by NP contribution. The parameter A , usually constrained by $|V_{cb}|$, is constrained here by the combination of Δm_d , Δm_s , and ϵ_K , processes which also constrain the r parameter.

It can be seen on Fig. 3.3 that it is $|V_{cb}|$, and hence the parameter A , that brings the most important information on the fit for r . CMFV deviations from the SM of the order of forty percent become possible when this information is lost.

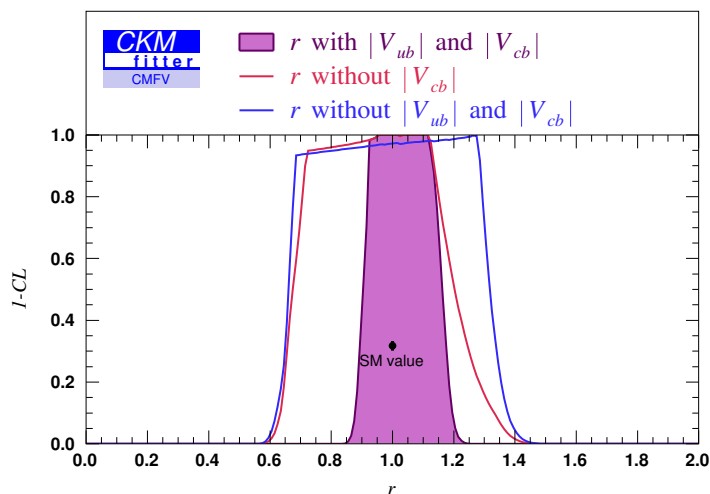


Figure 3.3: Fit for r using $|V_{ud}|$, $|V_{us}|$, $\sin 2\beta$, α , γ , Δm_d and Δm_s , and without $|V_{ub}|$ and $|V_{cb}|$ as inputs.

The fit for $|V_{ub}|$ in CMFV models, is shown in Fig. 3.4: the expected value is $|V_{ub}|_{\text{CMFV}} = (3.70 \pm 0.52)10^{-3}$, to be compared with $|V_{ub}|_{\text{SM}} = (3.70 \pm 0.12 \pm 0.26)10^{-3}$.

Since the (small) slope of the highest Confidence Level (CL) plateaus in Fig. 3.3 and Fig. 3.4 are inverted, it worth investigating the correlation between r and $|V_{ub}|$. This is shown in Fig. 3.5. The small correlation between r and $|V_{ub}|$ is indeed negative, and the allowed region includes the SM expectation.

A question arises at this stage: is it possible to cook a NP model working at tree level and satisfying the CMFV first assumptions (*i.e.* where flavour changing transition and CP violation only originate in the CKM matrix)?

A first attempt would be to add a new $SU(2)'_L$ broken gauge symmetry into the description, but a problem would appear with the Yukawa couplings.

Another attempt would be to implement a new $SU(2)_N$ acting only on the scalars, and whose mixing with $SU(2)_L$ would alter tree level amplitudes. However, fixing the effective G_F to its value from muon decay would fix all tree-level low energy processes to their SM value. To overcome this difficulty, one would be forced to venture into leptophobic models, so that NP would only affect quarks.

The implementation of the master function solely related to the mixing processes was the first step in implementing CMFV models into the framework of CKMfitter. To complete this work, one should include observables

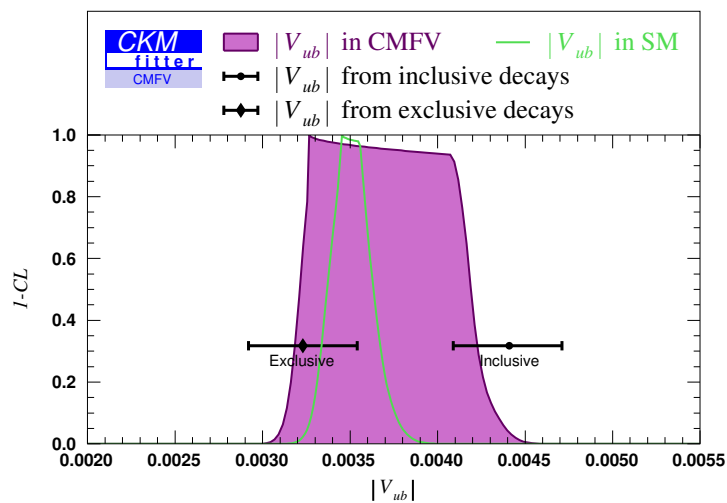
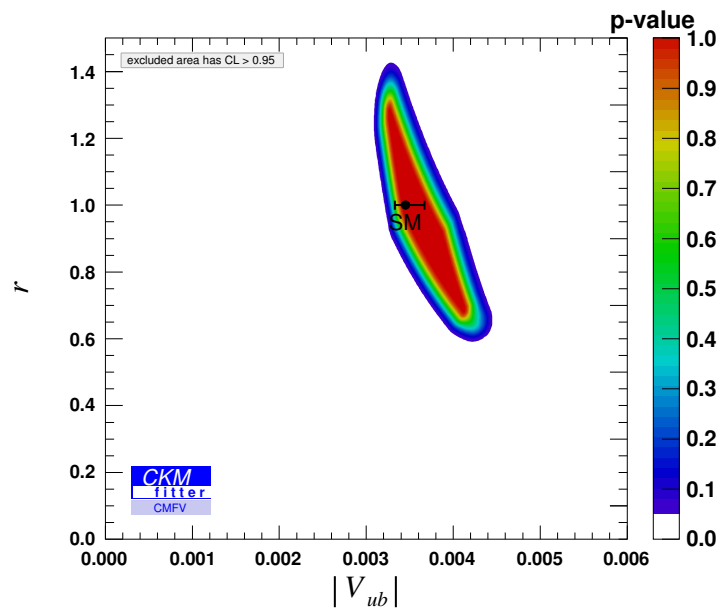


Figure 3.4: Prediction fit for $|V_{ub}|$ in CMFV models

depending on other CMFV master functions, adding new free parameters into the fit, as well as using new observables.

Figure 3.5: Correlation between r and $|V_{ub}|$.

Conclusion

To conclude, we have seen in this paper a way to introduce a Constrained Minimal Flavour Violation model into the CKMfitter package, as well as the effect of the new LHCb measurement of $B(B_s \rightarrow \mu^+ \mu^-)$ and ϕ_s on the $(\bar{\rho}_s, \bar{\eta}_s)$ plane. It is observed that the most important measurement as far as the null tests of Standard Model hypothesis are concerned is the ϕ_s measurement.

Secondly, it has been seen that slightly modifying the theory by adding a multiplicative free parameter in the $B_{d,s}^0 - \bar{B}_{d,s}^0$ and $K - \bar{K}$ mixing, order twenty percent CMFV contributions are allowed, going up to forty percent if New Physics appears at tree level. For the other processes, the implementation will be of the same type, adding in total 7 new free parameters to the Standard Model (more if New Physics appears at tree level).

The next step is to implement CMFV in the Next to Leading Order package, as well as including an additional parameter governing tree level amplitudes modifications, so that the parameters $|V_{ub}|$ and $|V_{cb}|$ could be included in the fit once again.

Eventually a complete CMFV analysis does require new observables to be introduced in order to constrain the other master function. This is a perspective made possible by the exploration work made in this document.

List of Figures

1.1	Unitary Triangle	6
1.2	Box and penguin diagrams.	7
2.1	Fit of $\bar{\rho}_s, \bar{\eta}_s$ using $ V_{cb} , V_{cs} $ and $B(B_s \rightarrow \mu\mu)$ as inputs.	10
3.1	Box diagram of a $\Delta F = 2$ transition.	13
3.2	Fit for r using $ V_{ud} , V_{us} , V_{ub} , V_{cb} , \sin 2\beta, \alpha, \gamma, \Delta m_d$ and Δm_s as inputs.	14
3.3	Fit for r using $ V_{ud} , V_{us} , \sin 2\beta, \alpha, \gamma, \Delta m_d$ and Δm_s , and without $ V_{ub} $ and $ V_{cb} $ as inputs.	16
3.4	Prediction fit for $ V_{ub} $ in CMFV models	17
3.5	Correlation between r and $ V_{ub} $	18

Bibliography

- [1] J. Goldstone, A. Salam, and S. Weinberg, “Broken Symmetries,” *Phys.Rev.*, vol. 127, pp. 965–970, 1962.
- [2] N. Cabibbo, “Unitary symmetry and leptonic decays,” *Phys. Rev. Lett.*, vol. 10, pp. 531–533, Jun 1963.
- [3] M. Kobayashi and T. Maskawa, “CP Violation in the Renormalizable Theory of Weak Interaction,” *Prog.Theor.Phys.*, vol. 49, pp. 652–657, 1973.
- [4] J. Beringer *et al.*, “Review of Particle Physics (RPP),” *Phys.Rev.*, vol. D86, p. 010001, 2012.
- [5] L. Wolfenstein, “Parametrization of the kobayashi-maskawa matrix,” *Phys. Rev. Lett.*, vol. 51, pp. 1945–1947, Nov 1983.
- [6] J. Charles, O. Deschamps, S. Descotes-Genon, R. Itoh, H. Lacker, *et al.*, “Predictions of selected flavour observables within the Standard Model,” *Phys.Rev.*, vol. D84, p. 033005, 2011.
- [7] A. J. Buras, “Minimal flavor violation,” *Acta Phys.Polon.*, vol. B34, pp. 5615–5668, 2003.
- [8] T. Inami and C. Lim, “Effects of Superheavy Quarks and Leptons in Low-Energy Weak Processes $K_L \rightarrow \mu\bar{\mu}$, $K^+ \rightarrow \pi^+\nu\bar{\nu}$, and $K^0 \leftrightarrow \bar{K}^0$,” *Prog.Theor.Phys.*, vol. 65, p. 297, 1981.
- [9] CMS and L. Collaborations, “Combination of results on the rare decays $B_{(s)}^0 \rightarrow \mu^+\mu^-$ from the CMS and LHCb experiments,” 2013.
- [10] A. Lenz, U. Nierste, J. Charles, S. Descotes-Genon, A. Jantsch, *et al.*, “Anatomy of New Physics in $B - \bar{B}$ mixing,” *Phys.Rev.*, vol. D83, p. 036004, 2011.

Abstract

The aim of the present work is to implement a Constrained Minimal Flavour Violation (CMFV) model into the $B_{d,s}^0$ and K^0 mixing processes. To do so, the use of an additional free parameter is needed to describe our theory. Adding this parameter, CMFV deviations of order between twenty or forty percent are allowed, depending whether New Physics appears or not at tree level.

Résumé

L'objectif du travail ici présent est d'implémenter un modèle de violation de saveur minimale contraint (CMFV) dans les processus de mélange $B_{d,s}^0$ et K^0 . Pour ce faire, un paramètre libre est utilisé afin de décrire notre théorie. En ajoutant ce paramètre, des déviations d'ordre vingt à quarante pourcent sont autorisées dans le cadre de CMFV, selon si la Nouvelle Physique apparaît à l'arbre ou non.